Characterization of activation energy for flow in metallic glasses

J. Q. Wang, W. H. Wang,* Y. H. Liu, and H. Y. Bai†

Institute of Physics, Chinese Academy of Sciences, Beijing 100190, P. R. China

(Received 21 August 2010; revised manuscript received 4 November 2010; published 10 January 2011)

The molar volume (V_m) scaled flow activation energy (ΔE), namely as the activation energy density $\rho_E = \Delta E/V_m$, is proposed to describe the flow of metallic glasses. Based on the energy landscape, both the shear and bulk moduli are critical parameters accounting for the ρ_E of both homogeneous and inhomogeneous flows in metallic glasses. The expression of ρ_E is determined experimentally to be a simple expression of $\rho_E = \frac{10}{11}G + \frac{1}{11}K$. The energy density perspective depicts a realistic picture for the flow in metallic glasses and is suggestive for understanding the glass transition and deformation in metallic glasses.

DOI: 10.1103/PhysRevB.83.012201 PACS number(s): 62.20.F−, 81.05.Kf

The desire to understand the mechanism of plastic deformation of bulk metallic glasses (BMG's) has caused much interest.[1–5] On the other hand, the mysterious glass transition phenomenon, which connects the liquid and glassy state, has wide applications in daily life, industry, and organism preservation.[6–8] In past decades, intensive efforts have been made to understand the glass transition and plastic deformation in metallic glasses.[1–6] Recently, it was certified that the thermodynamic origins of plastic deformation in BMG's and the glass transition are the same[4,5] and the glass transition, relaxation, and homogeneous and inhomogeneous deformations in glasses are all closely related to the flow event controlled by the activation energy barrier. It is therefore a major challenge to describe and model the homogeneous and inhomogeneous flows in metallic glasses.

A number of models have been proposed to explain the flow in glasses.[1–3,6–10] In elastic models, the elastic modulus is often found to play an important role in the flow.[5–11] For example, both the shoving model[6] and cooperative shearing model[11] suggest that the flow activation energy (ΔE) is directly linked with shear modulus G. The correlations between glass transition temperatures and the elastic moduli for various metallic glasses also confirm the important role of elastic moduli in the flow of glasses.[5,12–18] However, more and more evidence has been found that the flow activation energy in glasses and glass-forming liquids is not only related to G. In fact, in the homogeneous flow of glass-forming liquids, according to the shoving model, a characteristic volume V_c is involved as: $\Delta E = GV_c$.[6] In the inhomogeneous flow of glasses, the activation energy of a flow event unit (shear transformation zone, STZ) also correlates with volume as $\Delta E_{\mathrm{STZ}} = (8/\pi^2)G\gamma_C^2\zeta\Omega$, where Ω is the volume of STZ and $\boldsymbol{\gamma}_C$ is the shear strain limit.[11] On the other hand, the elastic moduli scaled with molar volume (V_m) show better correlations with the thermal and mechanical properties for metallic glasses.[17–20] Thus the characteristic volume or bulk modulus could be an important parameter involved in the flow event in glass transition and in glass, and consider that the merely single elastic modulus, such as the shear modulus, could not exactly capture the whole experimental observations.[17,18]

In this Brief Report, based on the potential energy landscape concept, we derive an energy density perspective on flow in metallic glasses that is associated with both shear and bulk moduli. The analysis demonstrates that the activation energy for flow in metallic glasses and glass-forming liquids are determined by both shear and dilatation effects. The proposition is certified by the experiment for various metallic glasses. The physical origin of the extended elastic model is discussed.

The temperature dependence of the viscosity η of glass-forming liquids can be described by the equation[6]

$$\eta = \eta_0 \exp\left[\frac{\Delta E(T)}{RT}\right], \tag{1}$$

where $\boldsymbol{\eta}_0$ is a constant, $\Delta E(T)$ the specific activation energy for flow (in units of J/mol), and R the gas constant. The specific activation energy is a characteristic physical parameter for a glass system and represents the activation energy required for per mole atoms. Recently, it was found that the molar volume V_m plays a critical role in the thermal and mechanical properties for metallic glasses.[5,17–20] Thus we define the activation energy of a unit volume as the activation energy density (ρ_E)

$$\rho_E = \frac{\Delta E}{V_m}. \tag{2}$$

With the definition of ρ_E, one can rule out the vague characteristic volume as being involved in both homogeneous and inhomogeneous flows and directly relate the flow activation event to the elastic moduli.[6,9,11]

The energy landscape has been widely used to describe the complex inherent states or flow in liquid and glass.[6,11] In the energy landscape perspective, as shown in Fig. 1, every minima represents one inherent state. The transition from one minima to another represents a flow event. The activation energy ΔE for flow is assumed to be mainly elastic energy[6,21] and can be expressed in a harmonic form $\rho_E = \frac{1}{2}M\gamma^2$ by second-order Taylor expansion around the minima,[22] where M is the elastic moduli and γ the elastic strain. The equipartition law of statistical mechanics gives $\frac{1}{2}M\langle\gamma^2\rangle = \frac{1}{2}k_BT/V_m$,[23] suggesting that $\langle\gamma^2\rangle = k_BT/MV_m$. In the energy landscape, if the distance $2\gamma_0$ between the minima is constant, the real energy barriers will be proportional to the barrier estimated by second-order Taylor expansion (the thin curves in Fig. 1). The estimated flow activation energy density is $\rho_E = \frac{1}{2}M\gamma_0^2 = \frac{1}{2}\frac{k_BT}{\langle\gamma^2\rangle}\gamma_0^2$ or $\rho_E \propto \frac{k_BT/V_m}{\langle\gamma^2\rangle}$. Because the atoms

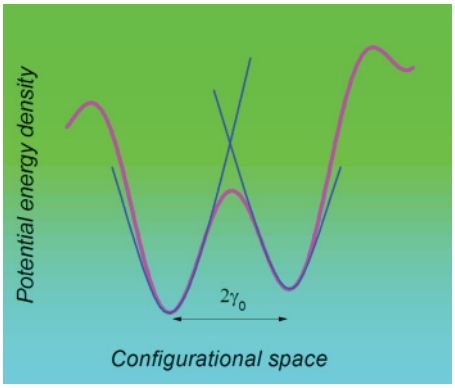

FIG. 1. (Color online) The pink full curve shows the schematic map of the potential energy density landscape with the distance $2\gamma_0$ between the minima. The blue thin curve gives the estimation by second-order Taylor expansions around the minima.

release three degrees of freedom around the glass transition,[24] one has $\langle\gamma^2\rangle = \frac{k_BT/V_m}{M_x} + \frac{k_BT/V_m}{M_y} + \frac{k_BT/V_m}{M_z}$, where x, y, and z represent the three directions in Cartesian coordinates and M_x, M_y, and M_z are the corresponding elastic moduli. For isotropic materials, they represent two shear moduli and one longitudinal modulus as $M_x = M_y = \rho V_S^2 = G$ and $M_z = \rho V_L^2 = K + 4G/3$, where ρ is the mass density, K the bulk modulus, and V_S and V_L are the shear and longitudinal sound velocities, respectively. Then one gets

$$\langle\gamma^2\rangle = \frac{2k_BT/V_m}{\rho V_S^2} + \frac{k_BT/V_m}{\rho V_L^2} = \frac{2k_BT/V_m}{G} + \frac{k_BT/V_m}{K + 4G/3}. \tag{3}$$

Substituting Eq. (3) into $\rho_E \propto \frac{k_BT/V_m}{\langle\gamma^2\rangle}$ gives $\rho_E \propto \frac{G(K+4G/3)}{2K+11G/3}$. The linear contribution of G and K can be estimated by defining the temperature dependency of ρ_E $I = \frac{d\ln\rho_E(T)}{d\ln T}$,[22] we get $I = (1 - \frac{KG}{2K^2+\frac{19}{3}KG+\frac{44}{9}G^2}) \bullet I_G + \frac{KG}{2K^2+\frac{19}{3}KG+\frac{44}{9}G^2} \bullet I_K$, alternatively, $I = (1-\alpha) \bullet I_G + \alpha \bullet I_K$, with

$$\alpha = \frac{KG}{2K^2 + \frac{19}{3}KG + \frac{44}{9}G^2}. \tag{4}$$

For metallic glasses, G/K varying from 0.2 to 0.5[4,20] gives the partition coefficient of $\alpha = 0.07 \pm 0.01$. The nonzero partition coefficient suggests that both the volume-conservative shearing (corresponding to G) and volume-nonconservative dilatation (corresponding to K) contribute to the flow of metallic glasses, and dilatation contributes around 7% to the activation energy density for creating the room for atomic rearrangement.[25]

To determine the exact contribution of K and G to the activation energy density for flow, the acoustic velocities change during glass transition has been studied. The T-dependent transversal (V_s) and longitudinal (V_L) velocities change differently during the glass transition process.[6,26] The ratio of the relative changes of the two velocities is about $\frac{\Delta V_S}{V_S} : \frac{\Delta V_L}{V_L} \approx 2:1$.[6,26] From $\rho V_S^2 = G$ and $\rho V_L^2 = \frac{4}{3}G + K$, we obtain the relative changes of G and K, $\frac{\Delta G}{G} : \frac{\Delta K}{K} \approx 5:1$. In three-dimensional space, there are two shear modes(corresponding to G) and one radial mode (dilatation mode corresponding to K) when atoms move. Thus the contribution of G should be doubled and the ratio of the

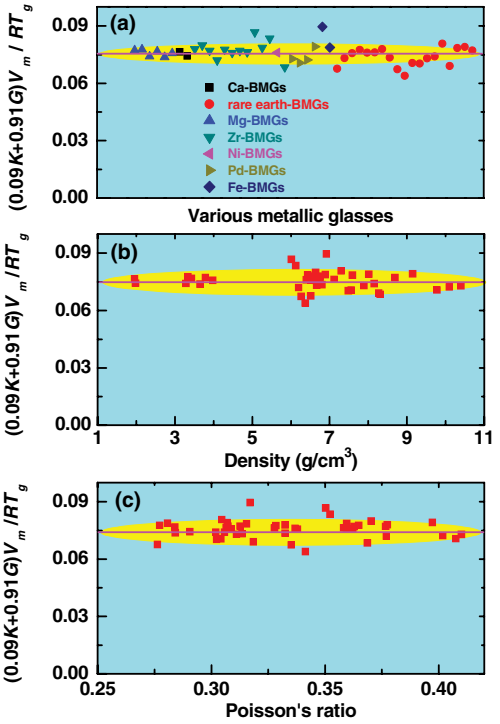

FIG. 2. (Color online) (a) The experimental data of $(0.91G + 0.09\ K)Vm/RTg$ versus various kinds of BMG's. (b) The $(0.91G + 0.09K)Vm/RTg$ versus mass density. (c) The $(0.91G + 0.09K)Vm/RTg$ versus ν. We can find that the $(0.91G + 0.09K)Vm/RTg$ is independent of materials and can be fitted by a constant very well.

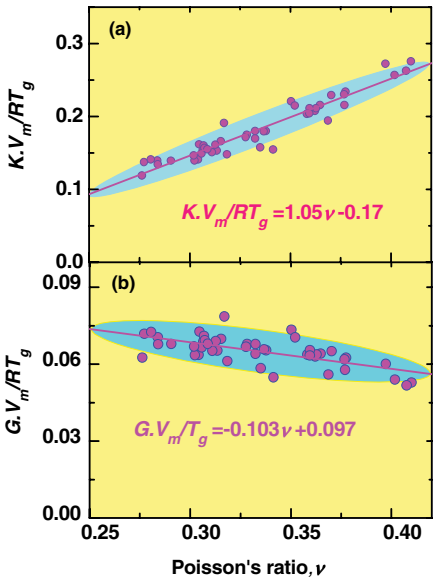

FIG. 3. (Color online) (a) The KVm/RTg and (b) GVm/RTg versus ν for 46 kinds of metallic glasses. The lines are the linear fit result of the experimental data. They have clear dependence on ν.

contribution of G and K in ρ_E should be about 10 : 1, that is,

$$\rho_E = \tfrac{10}{11}G + \tfrac{1}{11}K, \quad (5)$$

indicating $\alpha = 1/11 = 9\%$, which is consistent with the previous theoretical result.

To further confirm the model, we check the correlations between glass transition temperatures and the elastic moduli for various metallic glasses, which play a key role for verifying the elastic moduli for the flow of glasses.[12–18] Upon glass transition, the viscosity of glass-forming liquids approaches $\eta(T_g) = 10^{13}$ poise,[2,3] suggesting $\frac{\Delta E(T)}{RT}|_{T=T_g} \equiv$ constant.[1] Therefore, $\Delta E/T_g$ should be independent of the metallic glasses. According to our model, $\frac{\rho_E V_m}{RT_g} = \frac{(0.91G+0.09K)V_m}{RT_g} \equiv$ constant. Figure 2(a) shows the data of $\frac{(0.91G+0.09K)V_m}{RT_g}$ versus various kinds of BMG's (data are listed in Table I). One can see that these data can be fitted by a constant 0.075 very well. The data of $\frac{(0.91G+0.09K)V_m}{RT_g}$ for various metallic glasses versus other parameters such as density and Poisson's ratio are shown in

TABLE I. The compositions T_g, average molar volume V_m, ν, and the combined parameters $Moduli{\cdot}V_m/RT_g$ of 46 different kinds of BMG's (Refs. 14,15,20) are shown.

Compositions	T_g K	V_m cm^3/mol	ν	GV_m/RT_g	KV_m/RT_g	$(0.91G+0.09K)V_m/RT_g$
$Ca_{65}Mg_{8.54}Li_{9.96}Zn_{16.5}$	317	20.25	0.307	0.0688	0.155	0.0765
$Ca_{65}Mg_{8.31}Li_{9.69}Zn_{17}$	320	20.10	0.291	0.0678	0.139	0.0743
$Yb_{62.5}Zn_{15}Mg_{17.5}Cu_5$	385	19.24	0.276	0.0625	0.119	0.0676
$Ce_{70}Al_{10}Ni_{10}Cu_{10}$	359	16.94	0.314	0.0653	0.153	0.0732
$(Ce_{20}La_{80})_{68}Al_{10}Cu_{20}Co_2$	366	16.78	0.338	0.0654	0.180	0.0757
$Ce_{68}Al_{10}Cu_{20}Nb_2$	345	16.70	0.328	0.0678	0.175	0.0775
$(Ce_{80}La_{20})_{68}Al_{10}Cu_{20}Co_2$	355	16.69	0.337	0.0658	0.180	0.0760
$Ce_{68}Al_{10}Cu_{20}Co_2$	352	16.57	0.328	0.0668	0.172	0.0763
$Ce_{68}Al_{10}Cu_{20}Ni_2$	352	16.57	0.333	0.0678	0.180	0.0779
$Ce_{68}Al_{10}Cu_{20}Co_2$	351	16.44	0.333	0.0640	0.170	0.0735
$La_{60}Al_{20}Co_{20}$	477	15.96	0.335	0.0585	0.158	0.0674
$Pr_{55}Al_{25}Co_{20}$	509	15.07	0.341	0.0548	0.155	0.0639
$Dy_{55}Al_{25}Co_{20}$	635	14.27	0.304	0.0636	0.141	0.0706
$Tb_{55}Al_{25}Co_{20}$	612	14.15	0.302	0.0635	0.140	0.0704
$Ho_{55}Al_{25}Co_{20}$	649	13.85	0.311	0.0652	0.151	0.0730
$Er_{55}Al_{25}Co_{20}$	663	13.55	0.306	0.0665	0.149	0.0740
$Tm_{39}Y_{16}Al_{25}Co_{20}$	664	13.51	0.305	0.0726	0.162	0.0807
$Tm_{55}Al_{25}Co_{20}$	678	13.47	0.319	0.0612	0.148	0.0690
$Lu_{39}Y_{16}Al_{25}Co_{20}$	687	13.30	0.316	0.0699	0.166	0.0785
$Lu_{45}Y_{10}Al_{25}Co_{20}$	698	13.25	0.307	0.0710	0.160	0.0790
$Lu_{55}Al_{25}Co_{20}$	701	13.20	0.307	0.0693	0.157	0.0772
$Mg_{65}Cu_{25}Gd_{10}$	421	12.51	0.313	0.0689	0.161	0.0772
$Mg_{65}Cu_{25}Y_9Gd_1$	423	12.37	0.277	0.0718	0.137	0.0777
$Mg_{65}Cu_{25}Y_{10}$	419	12.36	0.302	0.0669	0.147	0.0741
$Mg_{65}Cu_{25}Y_8Gd_2$	420	12.23	0.284	0.0705	0.140	0.0767
$Mg_{65}Cu_{25}Y_5Gd_5$	422	12.05	0.284	0.0677	0.134	0.0737
$Mg_{65}Cu_{25}Tb_{10}$	415	11.95	0.309	0.0680	0.155	0.0758
$Zr_{64.13}Cu_{15.75}Ni_{10.12}Al_{10}$	640	11.68	0.377	0.0624	0.234	0.0779
$Zr_{65}Cu_{15}Ni_{10}Al_{10}$	652	11.65	0.37	0.0651	0.229	0.0799
$Zr_{61.88}Cu_{18}Ni_{10.12}Al_{10}$	651	11.51	0.377	0.0618	0.230	0.0770
$Zr_{55}Al_{19}Co_{19}Cu_7$	733	11.44	0.377	0.0579	0.216	0.0720
$Zr_{57}Nb_5Cu_{15.4}Ni_{12.6}Al_{10}$	687	11.44	0.365	0.0641	0.216	0.0777
$Zr_{57}Ti_5Cu_{20}Ni_8Al_{10}$	657	11.43	0.362	0.0629	0.207	0.0760
$(Zr_{59}Ti_6Cu_{22}Ni_{13})_{85.7}Al_{14.3}$	689	10.74	0.363	0.0637	0.211	0.0770
$Cu_{45}Zr_{45}Al_7Gd_3$	670	10.71	0.358	0.0637	0.204	0.0764
$Zr_{46.75}Ti_{8.25}Cu_{10.15}Ni_{10}Be_{27.25}$	622	10.21	0.35	0.0734	0.221	0.0867
$Zr_{48}Nb_8Cu_{12}Fe_8Be_{24}$	658	10.17	0.36	0.0654	0.211	0.0785
$Zr_{41}Ti_{14}Cu_{12.5}Ni_{10}Be_{22.5}$	625	9.79	0.352	0.0705	0.215	0.0835
$Ni_{45}Ti_{20}Zr_{25}Al_{10}$	733	9.61	0.359	0.0634	0.204	0.0760
$Cu_{60}Zr_{20}Hf_{10}Ti_{10}$	754	9.50	0.369	0.0559	0.194	0.0684
$Pd_{77.5}Cu_6Si_{16.5}$	633	8.74	0.41	0.0528	0.276	0.0729
$Pd_{64}Ni_{16}P_{20}$	630	8.29	0.408	0.0517	0.263	0.0707
$Pd_{40}Cu_{40}P_{20}$	590	7.98	0.402	0.0540	0.257	0.0723
$Pd_{39}Ni_{10}Cu_{30}P_{21}$	560	7.97	0.397	0.0601	0.272	0.0791
$Fe_{53}Cr_{15}Mo_{14}Er_1C_{15}B_6$	900	7.94	0.317	0.0734	0.191	0.0840
$Fe_{61}Mn_{10}Cr_4Mo_6Er_1C_{15}B_6$	930	7.48	0.281	0.0725	0.141	0.0787

Figs. 2(b) and 2(c). One can see that the data are independent with these parameters and can also be fitted by the constant of 0.075 very well. The experimental comparison further testifies to the previous model. As a comparison, Figs. 3(a) and 3(b) also show the plots of KV_m/T_g and GV_m/T_g versus ν. Fitting to the data yields $KV_m/T_g \propto 8.78\,\boldsymbol{\nu}$ and $GV_m/T_g \propto -0.86\,\boldsymbol{\nu}$, which indicates that the sole K or G cannot characterize the activation energy density well.

Most models for flow in glasses and supercooled liquids consider the case of simple shear, which involves only shear stress and a shear modulus. Our model suggests that both the homogeneous and inhomogeneous flows, on one hand, are the shearing process, and on the other hand, must generate free volume which is a form of dilatation (in fact, the shear-induced dilatation has been widely observed[8,22,25,27]), and demonstrates that both shear and free volume are important for flow in glass transition, and provides an intuitional picture of the flow of the atoms or atomic groups in glass or liquid. Furthermore, the formation of shear bands when the BMG's deform plastically is thought to be akin to the process of glass transition.[4,5] This means that both the shear[11] and the dilatation[27] could be involved in the formation of shear bands. The characterization of the flow activation energy sheds light on the fundamental issues of glass transition and plastic deformation in metallic glasses.

The discussion with J. C. Dyre and experimental assistance of D. Q. Zhao and R. J. Wang is appreciated. Financial support is from the NSFC (Grants No. 50731008 and No. 50621061) and MOST 973 (Grants No. 2007CB613904 and No. 2010CB731603).

*whw@iphy.ac.cn
†hybai@iphy.ac.cn

[1] F. Spaepen, Acta Metall. **25**, 407 (1977).
[2] A. S. Argon, Acta Metall. **27**, 47 (1979).
[3] M. H. Cohen and D. Turnbull, J. Chem. Phys. **31**, 1164 (1959).
[4] J. J. Lewandowski and A. L. Greer, Nature Mater. **5**, 15 (2006).
[5] Y. H. Liu, C. T. Liu, W. H. Wang, A. Inoue, T. Sakurai, and M. W. Chen, Phys. Rev. Lett. **103**, 065504 (2009).
[6] J. C. Dyre, Rev. Mod. Phys. **78**, 953, (2006).
[7] C. A. Angell, Science **267**, 1924 (1995).
[8] P. G. Debenedetti and F. H. Stillinger, Nature (London) **410**, 259 (2001).
[9] S. V. Nemilov, Russ. J. Phys. Chem. **42**, 2673 (1968).
[10] J. C. Dyre, Nature Mater. **3**, 749 (2004).
[11] W. L. Johnson and K. Samwer, Phys. Rev. Lett. **95**, 195501 (2005).
[12] B. Yang, C. T. Liu, and T. G. Nieh, Appl. Phys. Lett. **88**, 221911 (2006).
[13] W. H. Wang, P. Wen, D. Q. Zhao, and R. J. Wang, J. Mater. Res. **18**, 2747 (2003).
[14] W. H. Wang, J. Appl. Phys. **99**, 093506 (2006).
[15] J. Q. Wang, W. H. Wang, and H. Y. Bai, Appl. Phys. Lett. **94**, 041910 (2009).
[16] S. V. Nemilov, J. Non-cryst. Solids **352**, 2715 (2006).
[17] M. Q. Jiang and L. H. Dai, Phys. Rev. B **76**, 054204 (2007).
[18] T. Egami, S. J. Poon, Z. Zhang, and V. Keppens, Phys. Rev. B **76**, 024203 (2007).
[19] D. Ma, A. D. Stoica, and X.-L. Wang, Appl. Phys. Lett. **91**, 021905 (2007).
[20] J. Q. Wang, W. H. Wang, H. B. Yu, and H.Y. Bai, Appl. Phys. Lett. **94**, 121904 (2009).
[21] J. D. Eshelby, Proc. R. Soc. London **241**, 376 (1957).
[22] J. C. Dyre and N. B. Olsen, Phys. Rev. E **69**, 042501 (2004).
[23] E. S. R. Gopal, *Speicific Heats at Low Temperatures* (Plenum Press, New York, 1966).
[24] H. B. Ke, P. Wen, D. Q. Zhao, and W. H. Wang, Appl. Phys. Lett. **96**, 251902 (2010).
[25] M. L. Falk, Phys. Rev. B **60**, 7062 (1999).
[26] B. Zhang, H. Y. Bai, R. J. Wang, Y. Wu, and W. H. Wang, Phys. Rev. B **76**, 012201 (2007).
[27] F. Spaepen, Nature Mater. **5**, 7 (2006).